

EFFECTS OF OPEN AND CLOSED DIVERTOR GEOMETRIES ON PLASMA BEHAVIOR IN DIII-D

T.W. Petrie,¹ N.S. Wolf,² M.E. Fenstermacher,² G.D. Porter,²
 S.L. Allen,² N.H. Brooks,¹ A.W. Hyatt,¹ R.J. La Haye,¹ C.J. Lasnier,²
 A.W. Leonard,¹ M.A. Mahdavi,¹ T.H. Osborne,¹ M.J. Schaffer,¹
 J.G. Watkins,⁴ W.P. West,¹ and the DIII-D Team

¹General Atomics, P.O. Box 85608, San Diego, California 92138-9784, USA

²Lawrence Livermore National Laboratory, Livermore, California, USA

³Sandia National Laboratories, Albuquerque, New Mexico, USA

Baffled (“closed”) divertors are designed to reduce the chance of recycling neutrals from leaking back into the core plasma. This is particularly effective when baffling is combined with particle pumping. This in turn results in a reduction of both pedestal and line-averaged densities of the core plasma, and offers opportunity for “advanced tokamak” operation, such as efficient current drive and access to favorable energy confinement regimes. Both modeling and experimental results from DIII-D have demonstrated the effectiveness of the closed divertor in preventing recycled neutrals from returning to the core. For example, a reduction of 2–2.5 in core ionization favoring closed diverted plasmas has been reported [1,2] for high triangularity H-mode plasmas at about one-half the Greenwald density [3].

The effects of divertor closure on the fueling rate, divertor detachment, and impurity content of high-triangularity, ELMy H-mode plasmas are examined. We find that (1) open versus closed geometry does not appear to play a major role in the evolution of several characteristic plasma parameters during gas puffing, such as the pedestal and separatrix densities at the onset of detachment, (2) the deuterium core fueling was modestly lower ($\approx 15\text{--}20\%$) in the closed divertor configuration, and (3) the closed divertor had less carbon than the open divertor at the same line-averaged density and power input, typically 15–30% less.

In this paper the performance of the DIII-D closed divertor is evaluated for deuterium-fueled plasmas for higher densities than those discussed above. In particular, we will be comparing divertor detachment, fueling rates, and impurity content in the plasma core for open and closed divertor configurations, as shown in Fig. 1(a,b). The upper divertor has two baffles: an outer baffle and a second (“dome”) baffle which largely separates the inboard and outboard divertor legs [4]. For discussion we will refer to this divertor as *closed* [Fig. 1(a)], and refer to the lower divertor, which does not have this baffling, as *open* [Fig. 1(b)]. Since high-triangularity plasmas in the open divertor cannot be actively pumped (unlike those in the closed divertor), we limit this study to *unpumped*, ELMing H-mode discharges. The plasmas considered in this study were characterized by: $I_p = 1.37$ MA, $q_{95} = 4.1$, $P_{\text{INPUT}} = 3.0\text{--}7.5$ MW, $n_e/n_{\text{GW}} \approx 0.6\text{--}0.8$, and triangularity of the X-point = 0.74.

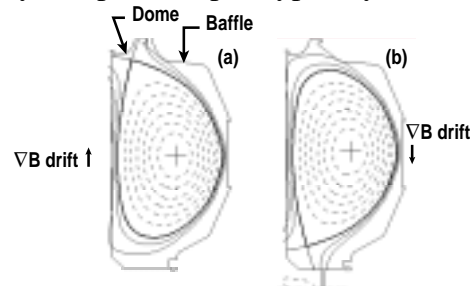


Fig. 1. The *closed* and *open* divertor geometries considered in this paper are shown in Figs. 1(a) and 1(b), respectively. For either case, the ∇B ion particle drift was toward the X-point. The 2 and 4 cm flux surfaces in the scrape-off layer (as measured at the midplane) are also shown. Unless otherwise denoted, the plasmas discussed are characterized by: $I_p = 1.37$ MA, $B_T = 2$ T, $q_{95} = 4.1$, $P_{\text{INPUT}} = 5$ MW, $Z_{\text{eff}} \leq 1.6$, and triangularity with respect to the X-point ≈ 0.74 . Sawtooth activity was observed in all discharges.

The temporal behavior of several global and edge discharge properties were only slightly affected by divertor baffling geometry during gas puffing. Figure 2 compares the evolution of a plasma discharge with a closed divertor against a similarly-prepared discharge with an open divertor. The temporal behavior of both line-averaged density, normalized to the Greenwald density, and the plasma stored energy tracked each other fairly closely [Fig. 2(c,d)], and the

ratio \bar{n}_e/n_{GW} at the termination of the H-mode (i.e., at the H-L back transition) was virtually the same. Edge plasma properties, such as pedestal density and electron temperature, also had very similar evolution for both shots [Fig 2(e,f)].

The relationship between pedestal density $n_{e,ped}$ and pedestal electron temperature $T_{e,ped}$ was insensitive to divertor closure [Fig. 3(a)]. For either open or closed diverted high density cases, gas puffing initially produced a pronounced decrease in $T_{e,ped}$ but little change in $n_{e,ped}$, also implying a sharp degradation in the electron pedestal pressure ($P_{e,ped}$). Figure 3(b) shows that a decrease in the energy confinement time (normalized to the ITER89P energy confinement time [5]) of a highly radiative zone at (or inside) coincided with this drop-off in $T_{e,ped}$ (and $P_{e,ped}$), and was consistent with the profile “stiffness” in electron temperature reported previously for gas puffed plasmas [6,7]. The energy confinement “trajectories” in $n_{e,ped}$ -ITER89P space were also insensitive to divertor closure. Similar results to the above were observed when the experiment was repeated at the 3.0 and 7.5 MW power levels.

“Partial detachment” of the divertor plasma is defined here as zero particle flux at the outer target near the separatrix (between ELMs). As with the low triangularity (δ) DIII-D plasma cases discussed elsewhere [8-11], detachment of the outer leg in both open and closed high- δ divertor cases occurred first at the separatrix strike point and then moved outward. Unlike typical low- δ DIII-D plasma cases [9,11], however, partial detachment was a gradual process at high- δ , as opposed to a rapid transition, and, more importantly, significant degradation in the stored energy was observed *prior* to detachment, as shown in Fig. 2(d). (Since we observe energy confinement degradation in both open and closed diverted discharges in this study, it is unlikely that this behavior in energy confinement can be tied directly to the divertor closure.) The formation of a highly radiative zone at (or inside)

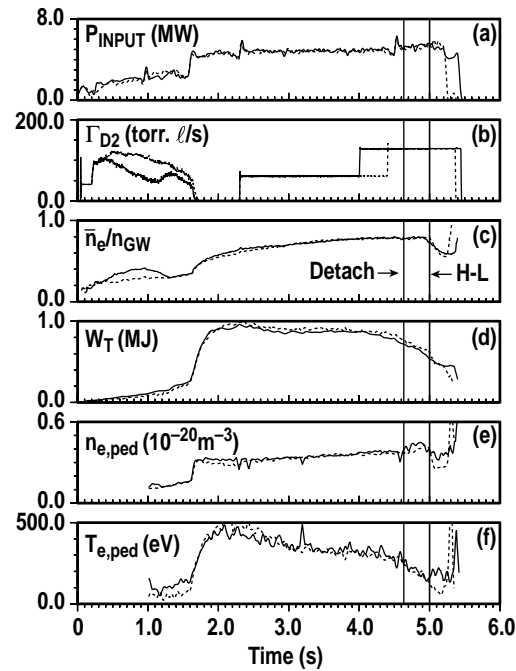


Fig. 2. Comparison of closed (shot 101560—solid curves) and open (shot 102447—dashed curves) diverted plasmas under similar power input (a) and gas puffing (b) programs. The timeslices for detachment of the outboard separatrix strike point, as well as the timeslices for their H-L back transition (Section 3), are denoted by the solid vertical lines. The evolutions of the line-averaged density, normalized to the Greenwald density n_{GW} (c), and of the plasma stored energy (d) tracked each other closely. The energy confinement, normalized to ITER89P L-mode scaling, was ≈ 2.0 just prior to the start of gas puffing ($t=2.3$ s) and was ≈ 1.4 just prior to detachment at $t \approx 4.65$ s. Pedestal density $n_{e,ped}$ (e) and electron temperature $T_{e,ped}$ (f) also shared similar temporal behaviors.

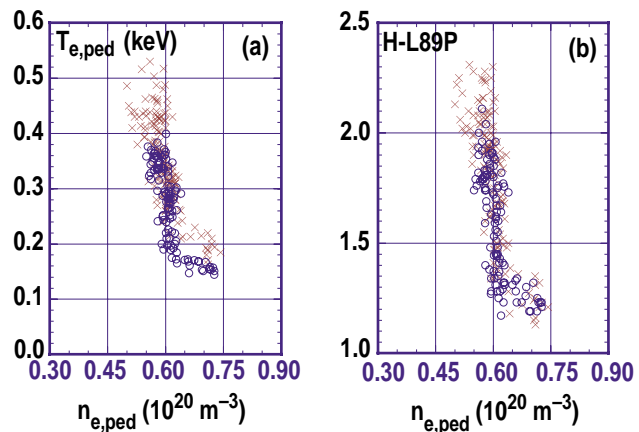


Fig. 3. (a) The variation of $T_{e,ped}$ with $n_{e,ped}$ was insensitive to whether the divertor was open (open circles) or closed (X's) during gas puffing. (b) The variation of energy confinement time (normalized to the ITER89P L-mode confinement time) with $n_{e,ped}$ was also insensitive to whether the divertor was open or closed. Partial detachment (Section 3) occurred at $n_{e,ped} = 0.61 \times 10^{20} \text{ m}^{-3}$ ($0.61 \times 10^{20} \text{ m}^{-3}$), $T_{e,ped} = 250 \text{ eV}$ (210 eV), and $H-L89P = 1.45$ (1.33) in the closed (open) configuration. The data are from several shots described by the parameters in the caption to Fig. 1.

the X-point separatrix was nearly coincident with the onset of partial detachment, similar to that previously observed in high density, low triangularity plasmas [12]. A rise in $n_{e,ped}$ and slight additional reduction in $T_{e,ped}$ [Fig. 2(e,f)] was observed following the onset of partial detachment, which normally took place near the “break” in the $T_{e,ped}$ and energy confinement curves [Fig. 3(a,b)].

Partial detachment occurred at the same pedestal density ($n_{e,ped,det}$) for both open and closed divertors for the three power levels used in this study (Fig. 4). This is also true for the upstream density along the separatrix ($n_{e,sep,det}$). That the ratio of $n_{e,ped,det}/n_{e,sep,det}$ is independent of divertor closure is addressed below.

Core fueling was lower for the closed divertor than for the open divertor, given the same density (e.g., $\bar{n}_e/n_{GW} \geq 0.72$), gas puff rate, energy confinement time, and power level. To understand this, the 2-d fluid plasma code UEDGE [13] was used to model two similar high density “attached” discharges under open and closed divertor geometry. The effect of the walls on the fuel particle balance was simulated by assuming surfaces in the divertor region below the X-point of both discharges were saturated (and therefore had a recycling coefficient of one), and wall surfaces elsewhere were assumed to have a recycling coefficient of 0.95. We also assumed for both open and closed divertor cases that $\chi_e = \chi_i = 0.3 \text{ m}^2/\text{s}$ and $D_{\perp} = 0.075 \text{ m}^2/\text{s}$. The plasmas were characterized by $P_{INPUT} = 4.9 \text{ MW}$, H-L89p = 1.85, and $\bar{n}_e/n_{GW} \approx 0.74$.

UEDGE calculates that the core deuterium fueling rate was $\approx 15\text{--}20\%$ lower in the closed divertor case in comparison with the corresponding open divertor case. This result is consistent with an independent approach based on the evolution of the radial profiles of the core density and temperature, as described by Porter [14]. From UEDGE analysis the recycling current in the closed divertor case was roughly twice that of the open divertor case. However, the contribution of this higher recycling current was offset by greater divertor screening, and thus a lower probability ($\approx 40\%$ that of the open divertor case) of these neutrals returning to fuel the core. The net fueling rate of the core, which is the product of these two factors, was then about 15–20% lower in the closed divertor case. In the UEDGE analysis of the closed divertor case the electron temperature was high enough to efficiently ionize recycling neutrals between the X-point and the divertor target.

It is noteworthy that, since $n_{e,ped,det}/n_{e,sep,det}$ was essentially the same for corresponding open and closed diverted discharges, significant core fueling for both cases could be expected to originate in the same general poloidal region. It has been shown previously [15] that ratio is sensitive to flux expansion at the location of a poloidally localized particle source. Additional support for a common poloidal location in peak fueling also comes from UEDGE analysis which indicates that the largest neutral source for both open and closed divertor cases is localized at or slightly above the X-point [Fig. 5(a)].

In the parameter range $\bar{n}_e/n_{GW} \approx 0.6\text{--}0.7$ and $P_{INPUT} = 3.0\text{--}7.5 \text{ MW}$, the carbon density in the core plasma was found to be $\approx 15\text{--}30\%$ higher in the open divertor cases than in the closed divertor cases, given comparable density and power input. Carbon content in the plasma core for either case, however, was low (i.e., $Z_{eff} \leq 1.6$). Preliminary UEDGE modeling agrees with lower core carbon density for the closed divertor. The transport assumptions were identical to those enumerated above; the source of carbon is assumed to be chemical and physical sputtering from the divertor plates and vessel walls [16]. Further details of the assumptions used in the modeling are given in Ref. [2].

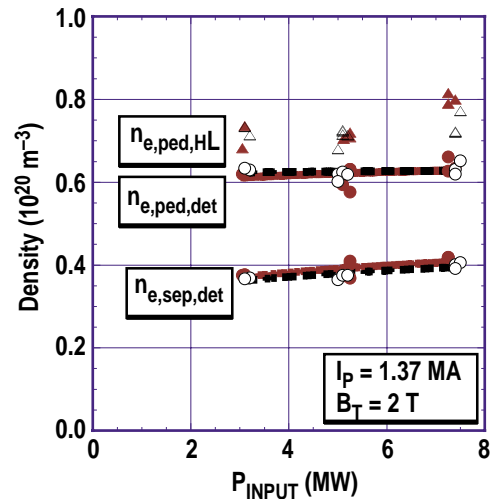


Fig. 4. The pedestal ($n_{e,ped,det}$) and separatrix ($n_{e,sep,det}$) densities immediately prior to detachment are shown for the open divertors (open circles) and closed (closed circles) divertors. Divertor closure did not appear to have a measurable effect on either $n_{e,ped,det}$ or $n_{e,sep,det}$, both of which depended only weakly on power input. The pedestal densities at the H-L back transition ($n_{e,ped,HL}$) are also shown for the open divertor (open triangles) and closed divertor (closed triangles) cases.

UEDGE modeling indicates that both baffles of the closed divertor reduced the probability of scattered carbon impurity escaping the divertor, either through the private flux region toward the X-point or out between the scrape-off layer and the vessel wall. The net result for the closed divertor case was lower carbon density near the X-point and upstream along the separatrix. This, in turn, ultimately led to fewer carbon ions diffusing into the core. For example, Fig. 5(b) shows the radial flux of C^{4+} into the core of the open and closed divertor cases; C^{4+} was the main carbon ion along the separatrix flux surface, where $T_e \approx 50\text{--}100\text{ eV}$. Thus, the restricted range of carbon impurities in the closed divertor region was a factor in lowering carbon ion flux along the scrape-off layer and reducing C^{4+} flux into the core above the X-point.

With regard to the carbon content in the core, factors other than geometry that could also play a role are: (1) newer tiles installed in the closed divertor and (2) better contouring of the tiles under the inboard leg of the closed divertor, hence, less edge heating and tile erosion at the tile edge. However, we have no experimental evidence that having flat tiles at the strike point on the inner wall contributed more core carbon than having the strike point on contoured tiles [17]. UEDGE results show that our carbon content observations are consistent with what is expected from purely geometrical considerations.

Although there were many similarities in the behavior of closed and open diverted discharges, modest differences in their deuterium core fueling were observed during deuterium gas puffing. The deuterium core fueling rate was slightly lower for the closed divertor configuration. UEDGE modeling indicated that the increased recycling current in the closed divertor was more than offset by the improved divertor screening of the recycled particles returning to the core. It is also important to note that the poloidal location of these fueling peaks for the baffled divertor case is well outside the “closed” divertor region. We speculate that the proximity to the X-point of an unbaffled region of high recycling (i.e., the inboard leg) may in part account for the reduced effectiveness in controlling core ionization in the “closed” divertor during gas puffing, and may hold the key to understanding the similarity in plasma behavior we have documented.

Work supported by U.S. Department of Energy under Contracts DE-AC03-99ER54463, W-7405-ENG-48, DE-AC05-00OR22725, and DE-AC04-AL85000.

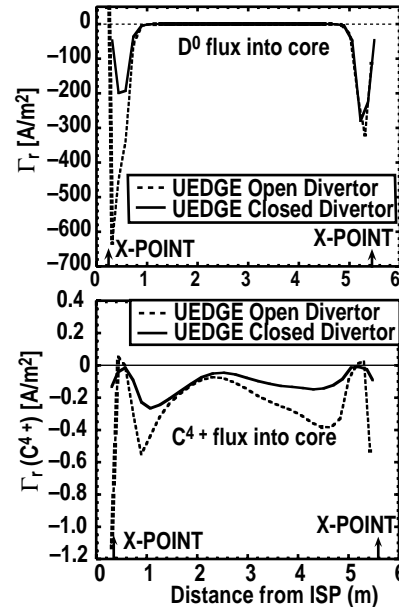


Fig. 5. The radial fluxes (a) of neutral deuterium and (b) of C^{4+} are shown as a function of poloidal distance along the separatrix from the inner strike point (ISP) to the outer strike point for both open and closed divertor cases. UEDGE analysis shows the larger radial flux is C^{4+} into the core of the open divertor.

- [1] S.L. Allen, et al., *J. Nucl. Mater.* **266-269** (1999) 168.
- [2] G.D. Porter, et al., *J. Nucl. Mater.* **290-293** (2001) 692.
- [3] M. Greenwald, et al., *Nucl. Fusion* **30** (1990) 1035.
- [4] S.L. Allen, et al., *J. Nucl. Mater.* **290-293** (2001) 995.
- [5] P.N. Yushmanov, et al., *Nucl. Fusion* **30** (1990) 1999.
- [6] W. Sutrop, et al., *Plasma Phys. Controlled Fusion* **39** (1997) 2051.
- [7] T.H. Osborne, et al., *Phys. Plasmas* **8** (2001) 2017.
- [8] T.W. Petrie, et al., in *Controlled Fusion and Plasma Physics (Proc. 18th Eur. Conf. Berlin, 1991)*, Vol. 15C, Part III, European Physical Society, Geneva (1991) 237.
- [9] T.W. Petrie, et al., *J. Nucl. Mater.* **196-198** (1992) 848.
- [10] T.W. Petrie, A.G. Kellman, M.A. Mahdavi, *Nucl. Fusion* **33** (1993) 929.
- [11] T.W. Petrie, et al., *Nucl. Fusion* **37** (1997) 321.
- [12] T.W. Petrie, et al., *J. Nucl. Mater.* **241-243** (1997) 639.
- [13] T.D. Rognlien, et al., *Contr. Plasma Phys.* **34** (1994) 362.
- [14] G.D. Porter and the DIII-D Team, *Phys. Plasmas* **5** (1998) 4311.
- [15] M.A. Mahavi, et al., “High Density H-mode Plasmas at Densities Above the Greenwald Limit,” Accepted for publication in *Nucl. Fusion*.
- [16] J.W. Davis and A.A. Haasz, *J. Nucl. Mater.* **241-243** (1997) 37.
- [17] C. J. Lasnier (private communication, 2001).